

Dynamical Structure Functions, Collective Modes, and Energy Gap in Charged-Particle Bilayers

Z. Donkó,¹ G. J. Kalman,² P. Hartmann,¹ K. I. Golden,³ and K. Kutasi¹

¹*Research Institute for Solid State Physics and Optics of the Hungarian Academy of Sciences, P.O. Box 49, H-1525 Budapest, Hungary*

²*Department of Physics, Boston College, Chestnut Hill, Massachusetts 02467, USA*

³*Department of Mathematics and Statistics and Department of Physics, University of Vermont, Burlington, Vermont 05401, USA*
(Received 12 June 2002; revised manuscript received 6 March 2003; published 3 June 2003)

The dynamical properties of strongly coupled charged-particle bilayers are investigated by molecular dynamics (MD) simulation and theoretical analysis. The spectra of the current correlation functions show the existence of two (in-phase and out-of-phase) longitudinal and two (in-phase and out-of-phase) transverse collective modes. The out-of-phase modes possess finite frequencies at wave numbers $k \rightarrow 0$, confirming the existence of the predicted long-wavelength energy gap in the bilayer system. A theoretical model based on an extended Feynman ansatz for the dynamical structure functions provides predictions on the strength of the collective modes that are verified by the MD experiment.

DOI: 10.1103/PhysRevLett.90.226804

PACS numbers: 73.21.-b, 05.20.-y, 52.27.Gr, 73.22.Lp

Strongly coupled charged-particle bilayers are relevant to supercooled ions in particle traps [1], semiconductor devices [2], and laboratory complex plasmas [3]. The dynamical properties of strongly coupled bilayers have been studied theoretically with the aid of the quasi-localized charge approximation (QLCA) [4]. The QLCA analysis has shown the existence of four distinct collective excitations [5]: the longitudinal in-phase and out-of-phase (particles in the two layers oscillating in phase and 180° out of phase, respectively) plasmon modes and the transverse in-phase and out-of-phase shear modes. The in-phase modes emulate a 2D behavior while the out-of-phase modes exhibit qualitatively new features. It has been predicted on the basis of the QLC theory that, in sharp contrast to the results of the RPA description where the long-wavelength out-of-phase plasmon is acoustic [6], this excitation exhibits a nonzero frequency at wave numbers $k \rightarrow 0$ [5]. New theoretical work [7] has addressed the questions of the structure of $S(\mathbf{k}, \omega)$, the dynamical structure function and the related issue of the spectral weight of the collective excitations. Experiments on the dispersion of the out-of-phase plasmon have been carried out in the low-coupling, high layer separation regime [2] (for a critical evaluation see also Ref. [8]). The possible relationship between these experimental findings, recent theoretical predictions, and the present molecular dynamics (MD) simulations will be discussed below.

In this Letter we report on MD calculation for bilayers in the strongly coupled liquid phase. Our goal here is to generate MD data for the dynamical structure functions and for the longitudinal and transverse current correlation functions, together with their companion dispersion relations. This classical simulation is also expected to reasonably well describe the qualitative features of col-

lective excitations of the strongly coupled bilayer in the quantum domain.

Our calculations are based on a P^3M (particle-particle particle-mesh) [9] molecular dynamics code, used earlier to investigate the static properties of the system [10]. The number of particles is set to $N = 1600$ in both layers, and periodic boundary conditions are applied to the simulation squares having an edge length D . The bilayer is isomorphic to a binary liquid with interaction potentials $\phi_{11}(r) = \phi_{22}(r) = e^2/r$ and $\phi_{12}(r) = \phi_{21}(r) = e^2/\sqrt{r^2 + \bar{d}^2}$ and is characterized by the coupling coefficient $\Gamma = e^2/(akT)$ and the layer separation $\bar{d} = d/a$, where $a = 1/\sqrt{n\pi}$ is the Wigner-Seitz radius, and n is the areal density.

Analyzing the dynamics of particles situated in layers $m = 1, 2$, data for $\lambda^{(m)}(k, t) = k \sum_i v_{ix}^{(m)} \exp[ikx_i^{(m)}]$, $\tau^{(m)}(k, t) = k \sum_i v_{iy}^{(m)} \exp[ikx_i^{(m)}]$, and $\rho^{(m)}(k, t) = \sum_i \exp[ikx_i^{(m)}]$ are stored for a series of wave numbers, multiples of $k_{\min} = 2\pi/D$. (We assume that \mathbf{k} is directed along the x axis.) Correlation functions of longitudinal (L_{ij}) and transverse (T_{ij}) current fluctuations and of density fluctuations (S_{ij}) are obtained through Fourier transforms of $\lambda(k, t)$, $\tau(k, t)$, and $\rho(k, t)$ [11,12]. The spectra are diagonalized by rotating them into a \pm coordinate system, e.g., $L_+(k, \omega) = L_{11} + L_{12}$ and $L_-(k, \omega) = L_{11} - L_{12}$.

Most of our calculations have been carried out for $\Gamma = 40$ and 60 , and layer separations in the $0.1 \leq \bar{d} \leq 5$ range. Figure 1 shows a series of representative longitudinal (L_+ and L_-) and transverse (T_+ and T_-) current and density (S_-) fluctuation spectra. In order to test the reliability of computation, we have calculated the zeroth and second frequency moments of $S_{\pm}(k, \omega)$. The former is compared with the static $S(k)$ obtained independently in our earlier work [10], the latter with the value required by the second

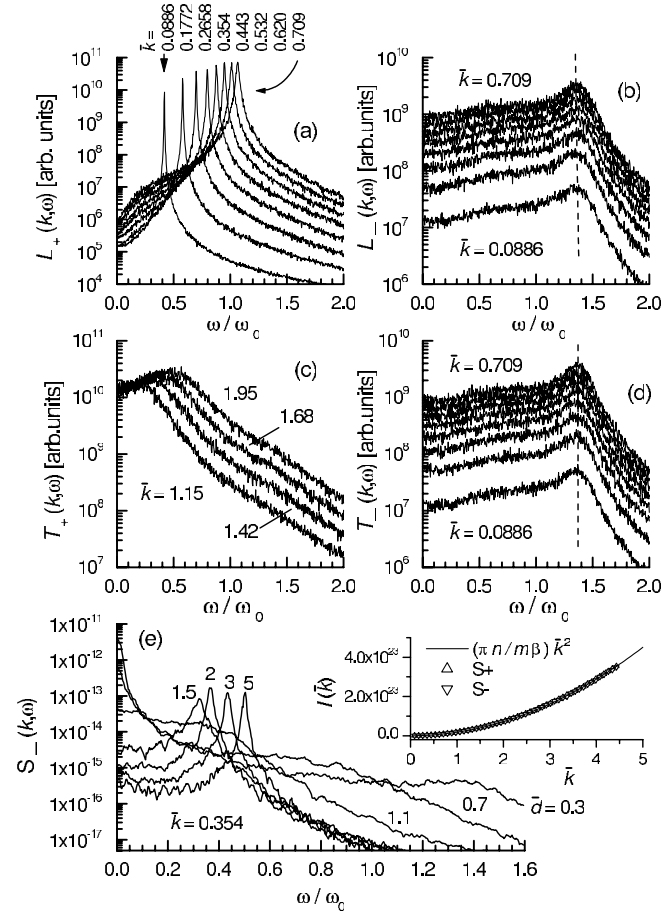


FIG. 1. Spectra of longitudinal $L_{\pm}(k, \omega)$ (a),(b) and transverse current $T_{\pm}(k, \omega)$ (c),(d) fluctuations at $\bar{d} = 0.3$; (e) $S_{-}(k, \omega)$ spectra for $\bar{d} = 0.3-5$; the inset illustrates the satisfaction of the second frequency moment sum rule; $I(\bar{k}) = \int \omega^2 S(k, \omega) d\omega$. $\Gamma = 60$ for (a)-(d); $\Gamma = 40$ for (e). $\omega_0 = \sqrt{2\pi e^2 n / ma}$ is the nominal 2D plasma frequency.

frequency moment sum rule, $(\pi n / m\beta) \bar{k}^2$ (where $\bar{k} = ka$ and $\beta = 1/k_B T$) [see inset in Fig. 1(e) showing excellent agreement]. The analysis of the correlation spectra confirms the existence of all four predicted collective modes. The full dispersion relations $\omega(k)$ at $\Gamma = 40$ and layer separation $\bar{d} = 0.3$ are plotted in Fig. 2(a). Both the longitudinal and transverse *out-of-phase* modes (\mathcal{L}_{-} , \mathcal{T}_{-}) show a weak dependence on the wave number k . As $k \rightarrow 0$ these modes exhibit a finite frequency $\omega(0) \neq 0$. This can also be observed in the positions of the peaks of the spectra in Figs. 1(b) and 1(d). This behavior provides unambiguous evidence for the presence of the predicted [5] energy gap in the out-of-phase mode spectrum of a strongly coupled bilayer.

In contrast, for the *in-phase* longitudinal mode (\mathcal{L}_{+}) ω shifts to 0 as $k \rightarrow 0$, as expected on the basis of the RPA dispersion of this mode, which is quasiacoustic $\omega/\omega_0 = \sqrt{2\bar{k}(1 - \bar{k}\bar{d}/2 + 3\bar{k}/4\Gamma)}$; $\omega_0 = \sqrt{2\pi e^2 n / ma}$. The QLCA predicts a further $O(k)$ correction due to correlations [5,6]; our data clearly confirm this deviation. The *in-*

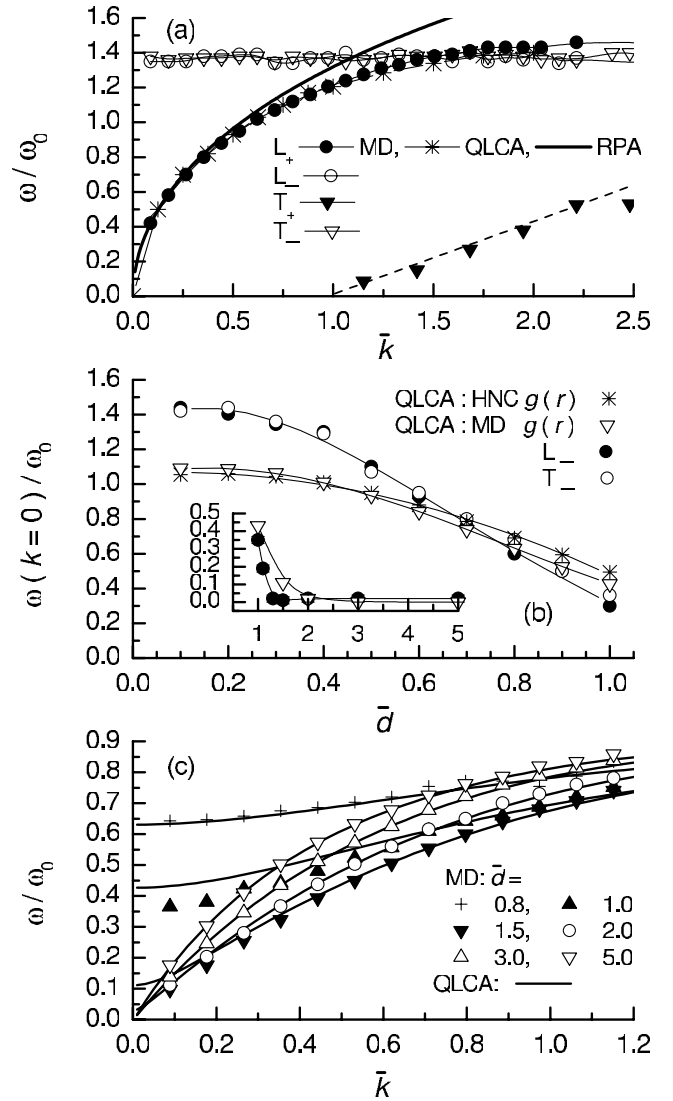


FIG. 2. (a) Dispersion relations for the four modes, at $\Gamma = 40$ and $\bar{d} = 0.3$; (b) energy gap $\omega(k=0)/\omega_0$ as a function of \bar{d} ; the inset portrays the high \bar{d} behavior; (c) dispersion of the \mathcal{L}_{-} mode for $\bar{d} = 0.8-5.0$. All data are compared with the results of the QLCA calculations [5]; (a) also shows the results of the RPA calculations.

phase transverse (\mathcal{T}_{+}) mode is similar to the corresponding mode in the isolated 2D system: for $\Gamma = 40$ it is quite weak and it is observable only at $\bar{k} \geq 1$; for $\bar{k} \leq 1$, $\omega = 0$. The disappearance of the shear modes for $k \rightarrow 0$ is a well-known feature of the liquid state [11,13,14] while the sharp cutoff $\omega \rightarrow 0$ for a finite k has also been observed in the case of Yukawa systems [15,16]. Comparison with the QLC theory shows an agreement as far as the linear acoustic dispersion is concerned, but the QLCA fails to predict the finite- k , $\omega = 0$ cutoff.

To see the effect of layer separation, the S_{-} spectra at fixed \bar{k} and the energy gap as functions of \bar{d} are shown in Figs. 1(e) and 2(b), respectively. The values of ω at $k \rightarrow 0$ for the \mathcal{L}_{-} and \mathcal{T}_{-} modes are coincident, as expected,

and show a decreasing tendency with increasing layer separation. At layer separations $d \rightarrow 0$, $\omega(k=0)/\omega_0 \approx 1.43$. Comparison with the QLCA gap formula [5] using pair correlation functions obtained from hypernetted-chain [5] and MD [10] calculations shows that the theoretical results are in good agreement with the MD data except that at small layer separations the latter is roughly 30% higher than the theoretical value. With increasing layer separation the energy gap value obtained from the simulations decreases faster than the QLC prediction, ultimately dropping below it (to 0.35) around $\bar{d} = 1$.

Focusing now further on the *longitudinal* (\mathcal{L}_-) mode for $\bar{d} \geq 1.5$, it is seen in Fig. 2(c) that the $\omega > 0$ portion of the dispersion curve following the energy gap is linear. It is in this domain that the mode bears a close resemblance to the behavior predicted by the RPA. The slope of this quasilinear portion is reduced by 66% (at $\bar{d} = 1.5$) to 39% (at $\bar{d} = 5$) from its RPA value due to the strong particle correlations.

The widths of the peaks in the fluctuation spectra are indicative of the lifetimes of the corresponding modes. \mathcal{L}_+ is maintained primarily by the mean field: it is characterized by a long lifetime and an extremely narrow peak in the corresponding $L_+(\omega)$ spectrum. In contrast, \mathcal{T}_+ and \mathcal{T}_- are supported by particle correlations, have shorter lifetimes, and are characterized by broader peaks in the $T_+(\omega)$ and $T_-(\omega)$ spectra. As to the peak of $L_-(\omega)$, it is broad in the domain dominated by correlations, in particular, in the gap region; it narrows dramatically, however, as it travels into the quasilinear region that is primarily maintained by the mean field [see Fig. 1(e)].

Our examination of the weaker coupling behavior indicates that the energy gap does survive even down to the $\Gamma = 5$ value; for $\Gamma < 5$ the corresponding peak becomes swamped by the continuum noise.

In order to analyze the features of the $S_{\pm}(k, \omega)$ structure functions we represent the ω dependence in terms of a Feynman-type ansatz:

$$S_{\pm}(k, \omega) = \pi(2p_{\pm}(k)\delta(\omega) + q_{\pm}(k)\{\delta[\omega - \omega_{\pm}(k)] + \delta[\omega + \omega_{\pm}(k)]\}). \quad (1)$$

The difference between Eq. (1) and the conventional Feynman representation resides in the zero frequency term. The introduction of this term is motivated by the observation that in multicomponent systems the hydrodynamic diffusion dominates the low frequency behavior and proper inclusion of this feature in $S(k, \omega)$ is indispensable. In contrast, in a single component plasma the central diffusion peak is suppressed at $k \rightarrow 0$ [10,11].

With the combination of (1) with compressibility sum rules specific to bilayers [7], one can establish precise statements in the $k \rightarrow 0$ limit on the integrated strengths both of the collective and of the central peaks over the entire $0 < T < \infty$ quantum to classical temperature range. Here we quote the classical limit. Each of the six

peaks exhibits its own characteristic k dependence, as shown in Fig. 3(a). The leading coefficients to $O(k^2)$ can be calculated in terms of the intralayer (L) and interlayer (N) inverse compressibilities [the additional factors γ_+ and g are of $O(1)$, and their precise values are of no interest here]:

$$\begin{aligned} P_{-}^{(0)} &= \frac{1}{L - N + 2\Gamma\bar{d}}, & P_{-}^{(1)} &= \frac{\Gamma\bar{d}^2}{[L - N + 2\Gamma\bar{d}]^2}, \\ Q_{-}^{(2)} &= \frac{1}{2\Gamma g^2}, & P_{+}^{(2)} &= [3 - (L + N) - 2\Gamma\gamma_+] \frac{1}{16\Gamma^2}, \\ Q_{+}^{(1)} &= \frac{1}{4\Gamma}, & Q_{+}^{(2)} &= [3 - 2\Gamma\gamma_+ - 2\Gamma\bar{d}] \frac{1}{16\Gamma^2}. \end{aligned} \quad (2)$$

We have performed a detailed MD analysis of the behavior of the central and collective peaks, focusing on verifying the predicted k and Γ dependences of the respective leading terms. The integration over the collective peak areas was carried out without difficulty, since

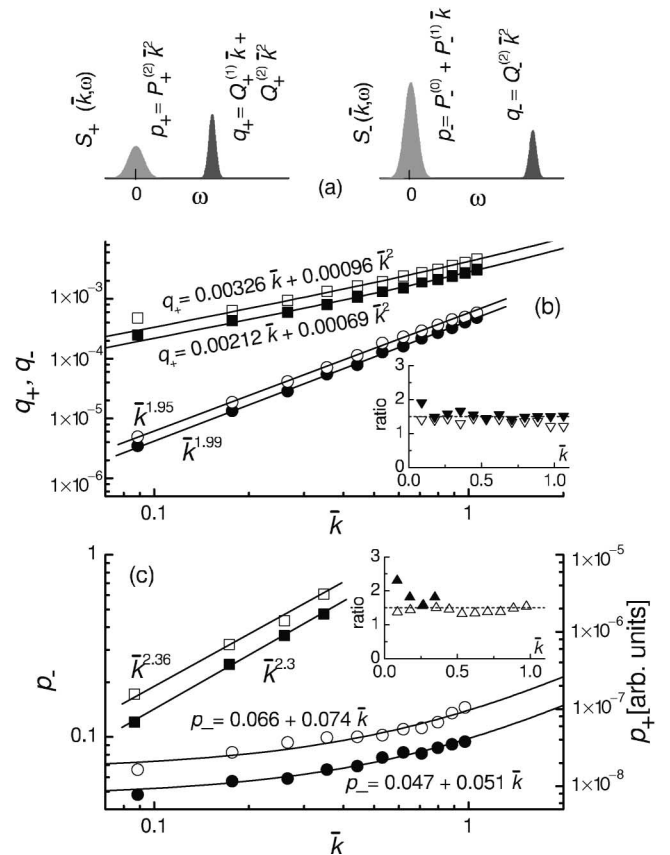


FIG. 3. (a) Qualitative picture for the \bar{k} dependences of the strengths of the central and the collective peaks; (b) collective peak strengths q_{+} (squares) and q_{-} (circles), and (c) central peak strengths p_{+} (squares) and p_{-} (circles) as functions of \bar{k} . Filled symbols: $\Gamma = 60$, open symbols: $\Gamma = 40$. Best fits for the coefficients $Q_{+}^{(1)}$ and $Q_{+}^{(2)}$ in q_{+} , and for $P_{-}^{(0)}$ and $P_{-}^{(1)}$ in p_{-} are displayed. For q_{-} and p_{+} the best fits for the power behavior of \bar{k} are displayed. The insets show the Γ dependences.

these peaks detach themselves sharply from the background. The central peaks are more diffuse, rendering the evaluation more difficult.

Figure 3(b) displays the results for the two collective peaks, q_+ and q_- . Both the theoretically required power behaviors (\bar{k} and \bar{k}^2 , respectively) and the inverse proportionality to Γ are verified. In addition, $Q_+^{(1)}$ has the correct value given by Eq. (2); $Q_+^{(2)}$ is, however, lower possibly because of damping effects. The analysis of p_+ and p_- [Fig. 3(c)] is more difficult because comparison with the theoretical values is hindered by the more complex Γ dependences through L and N , as predicted by Eq. (2). Nevertheless, the expected \bar{k} behaviors are well demonstrated. For large Γ values L and N are proportional to Γ [7]: thus an overall inverse proportionality with Γ is expected. This is also borne out in Fig. 3(c). For p_- we exploited the fact that $P_-^{(0)}$ is identical to the static structure function $S_-(k=0)$ [7] and that $P_-^{(1)}$ is expressible in terms of $P_-^{(0)}$. Borrowing the value of $S_-(k=0)$ from our earlier static simulation data [17], we have found reasonable numerical agreement between theoretically calculated and measured values of the coefficients, as indicated in Fig. 3(c).

The work of [18] suggested that the energy gap is only an artifice of the approximation used (QLCA) and the damping effects render its oscillator strength vanishingly small. The results presented here clearly show that this is not the case. The MD experiment that obviously includes all damping effects demonstrates that the gapped mode prevails as a well-defined and identifiable collective excitation of the system. From the theoretical side it is seen that while it is true that the strength of the collective peak in $S_-(k, \omega)$ is down by a factor of k , as compared to the collective peak of $S_+(k, \omega)$, this is a feature that would be shared by any competing pair of optic and acoustic or quasiaoustic excitations and is due merely to the different densities of states associated with the two modes.

In summary, we have presented MD simulation results for charge and current fluctuation spectra for a charged-particle bilayer liquid over a wide range of coupling and layer separation values. The dynamical structure function data well satisfy the required sum rules.

We have identified the four collective modes of the system and determined their dispersion characteristics: the existence of the predicted [5] frequency (energy) gap in the out-of-phase modes has been unambiguously established. The MD results on the mode dispersion well complement the existing experimental findings [2,8] in laboratory experiments: these latter were carried out for $r_s \approx 1.0-1.5$, equivalent to a much weaker coupling range than that investigated here. The high \bar{d} , finite- k region accessed by the experiments can be identified

with the quasilinear portion of the high \bar{d} dispersion curves in Fig. 2(c).

We have shown that the extended Feynman ansatz [Eq. (1)] provides a precise analytical determination of the long-wavelength behavior of the collective and $\omega = 0$ peaks of $S(k, \omega)$. We have measured the strengths of the respective peaks in the MD simulation and have demonstrated that they conform with the theoretical predictions based on this model.

We thank S. Hamaguchi, H. Gould, K. Blagoev, and S. Kyrkos for useful discussions. This work has been supported by Grants No. MTA-OTKA-NSF-28, No. OTKA-T-34156, No. NSF-INT-0002200, No. DE-FG02-98ER54501, No. DE-FG02-98ER54491, No. NSF-PHY-0206695, and No. NSF-PHY-0206554.

-
- [1] T. B. Mitchell, J. J. Bollinger, D. H. E. Dubin, X.-P. Huang, W. M. Itano, and R. H. Buntham, *Science* **282**, 1290 (1998).
 - [2] See, e.g., D. S. Kainth, D. Richards, H. P. Richards, M. Y. Simmons, and D. A. Ritchie, *J. Phys. Condens. Matter* **12**, 439 (2000).
 - [3] See, e.g., A. Melzer, V. A. Schweigert, I. V. Schweigert, A. Homann, S. Peters, and A. Piel, *Phys. Rev. E* **54**, R46 (1996).
 - [4] G. J. Kalman and K. I. Golden, *Phys. Rev. A* **41**, 5516 (1990); K. I. Golden and G. J. Kalman, *Phys. Plasmas* **7**, 14 (2000).
 - [5] G. J. Kalman, V. Valtchinov, and K. I. Golden, *Phys. Rev. Lett.* **82**, 3124 (1999).
 - [6] R. Z. Vitlina and A. V. Chaplik, *Zh. Eksp. Teor. Fiz.* **81**, 1011 (1981) [*Sov. Phys. JETP* **54**, 536 (1981)]; S. Das Sarma and A. Madhukar, *Phys. Rev. B* **23**, 805 (1981).
 - [7] K. I. Golden and G. J. Kalman, *J. Phys. A* **36**, 5865 (2003).
 - [8] P. G. Bolcatto and C. R. Proetto, *Phys. Rev. Lett.* **85**, 1734 (2000).
 - [9] R. W. Hockney and J. W. Eastwood, *Computer Simulation Using Particles* (McGraw-Hill, New York, 1981).
 - [10] Z. Donkó and G. J. Kalman, *Phys. Rev. E* **63**, 061504 (2001).
 - [11] J.-P. Hansen, I. R. McDonald, and E. L. Pollock, *Phys. Rev. A* **11**, 1025 (1975).
 - [12] S. Hamaguchi, *Plasmas and Ions* **2**, 57 (1999).
 - [13] H. Totsuji and N. Kakeya, *Phys. Rev. A* **22**, 1220 (1980).
 - [14] P. Schmidt, G. Zwicknagel, P.-G. Reinhard, and C. Toepffer, *Phys. Rev. E* **56**, 7310 (1997).
 - [15] H. Ohta and S. Hamaguchi, *Phys. Rev. Lett.* **84**, 6026 (2000).
 - [16] M. S. Murillo, *Phys. Rev. Lett.* **85**, 2514 (2000).
 - [17] G. J. Kalman *et al.*, *J. Phys. IV (Paris)* **10**, Pr5-85 (2000).
 - [18] J. Ortner, *Phys. Rev. B* **59**, 9870 (1999).